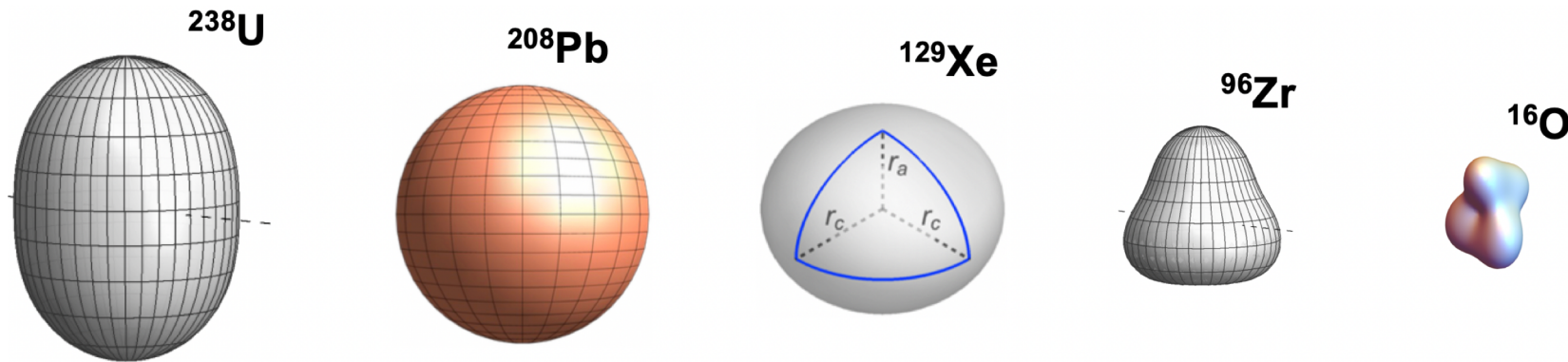




Intersection between nuclear structure and heavy-ion collisions

Jiangyong Jia and Giuliano Giacalone

Sept 3 - Sept 9, 2023



Stony Brook University

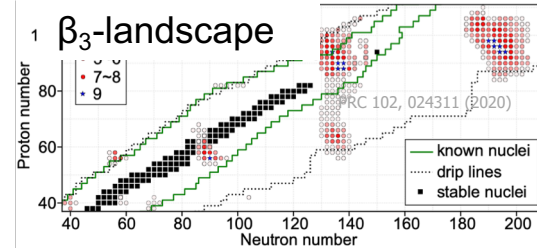
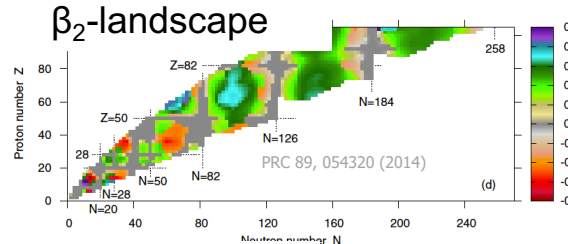
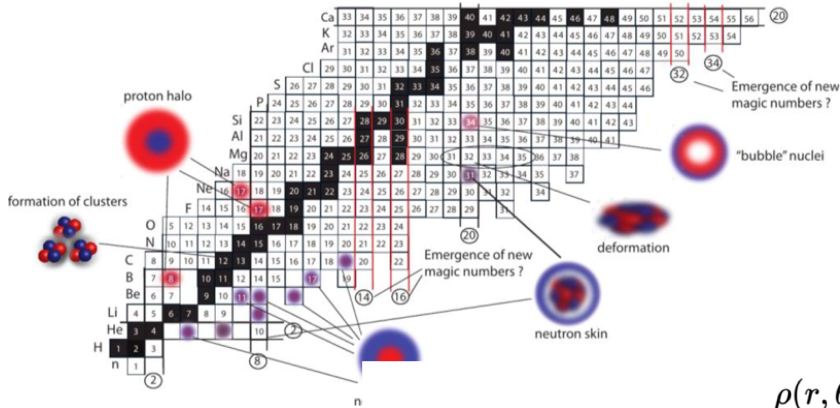
Quark Matter 2023



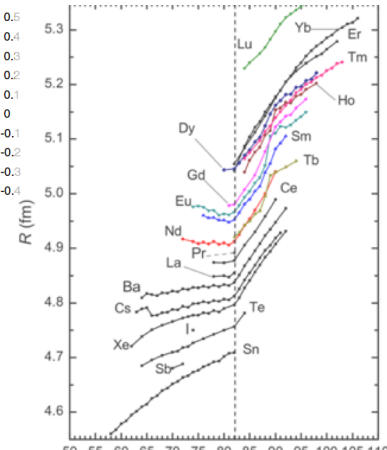
Collective structure of atomic nuclei

Emergent phenomena of the many-body quantum system

- clustering, halo, skin, bubble...
- quadrupole/octupole/hexadecapole deformations
- Non-monotonic evolution with N and Z

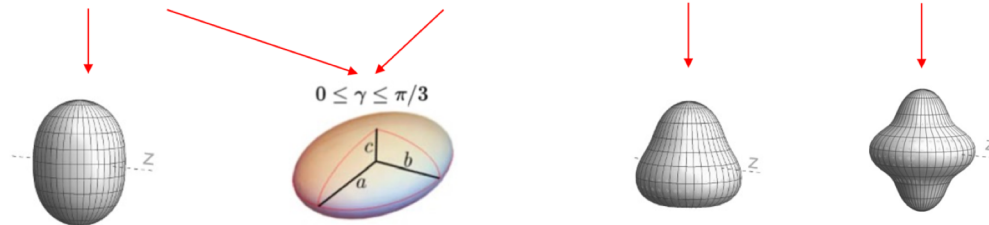
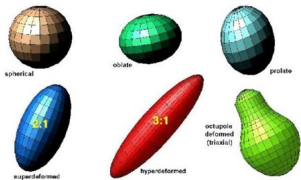


Radii-landscape



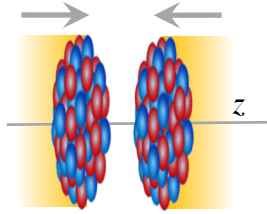
$$\rho(r, \theta, \phi) = \frac{\rho_0}{1 + e^{(r-R(\theta, \phi))/a_0}}$$

$$R(\theta, \phi) = R_0(1 + \beta_2[\cos \gamma Y_{2,0}(\theta, \phi) + \sin \gamma Y_{2,2}(\theta, \phi)] + \beta_3 Y_{3,0}(\theta, \phi) + \beta_4 Y_{4,0}(\theta, \phi))$$

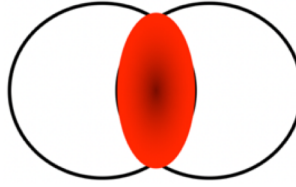


Role of nuclear structure in heavy ion collisions

Nuclear structure



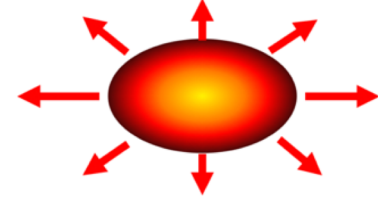
Initial condition



hydrodynamics



Final state



Status

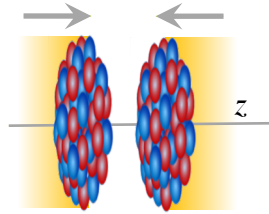
- Precision of QGP properties depends on initial condition and energy deposition
- Detailed nuclear structure information not yet part of hydro framework

Two-fold goal

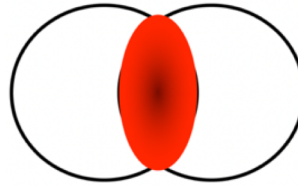
- **Constrain the initial condition** by comparing nuclei with known structure properties
- **Extract properties of nuclei** from heavy-ion collisions and compare to low-energy

Role of nuclear structure in heavy ion collisions

Nuclear structure



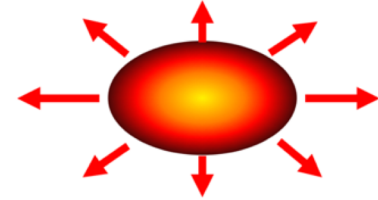
Initial condition



hydrodynamics



Final state



Shape and radial dis.

- $\beta_2 \rightarrow$ Quadrupole deformation
- $\beta_3 \rightarrow$ Octupole deformation
- $a_0 \rightarrow$ Surface diffuseness
- $R_0 \rightarrow$ Nuclear size

Volume, size and shape

$$\begin{aligned} N_{\text{part}} \\ R_{\perp}^2 &\propto \langle r_{\perp}^2 \rangle \\ \mathcal{E}_n &\propto \langle r_{\perp}^n e^{in\phi} \rangle \end{aligned}$$

Observables

$$\frac{d^2 N}{d\phi dp_T} = N(p_T) \left(\sum_n V_n e^{-in\phi} \right)$$

Anisotropic flow

Radial flow

linear response between initial and final state moments: $V_n \propto \mathcal{E}_n$

Initial shape

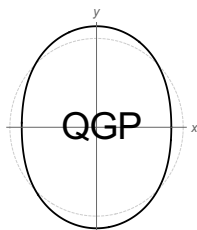
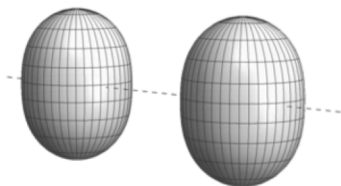
$$\frac{\delta[p_T]}{[p_T]} \propto -\frac{\delta R_{\perp}}{R_{\perp}}$$

Initial size

How initial condition is impacted by nuclear structure?

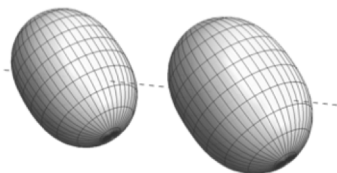
Connecting initial condition to nuclear shape

Body-Body



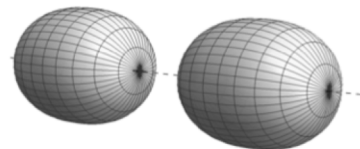
$$\epsilon_2 \sim 0.95\beta_2$$

$$\mathcal{E}_2 = \epsilon_2 e^{i2\Phi} \propto \langle \mathbf{r}_\perp^2 e^{i2\phi} \rangle$$



$$\epsilon_2 \sim 0.48\beta_2$$

Tip-Tip



$$\epsilon_2 \sim 0$$

$$\epsilon_2 = \underbrace{\epsilon_0}_{\text{undeformed}} + \underbrace{p(\Omega_1, \Omega_2)}_{\text{phase factor}} \beta_2 + \mathcal{O}(\beta_2^2)$$

Shape depends on Euler angle $\Omega = \varphi\theta\psi$

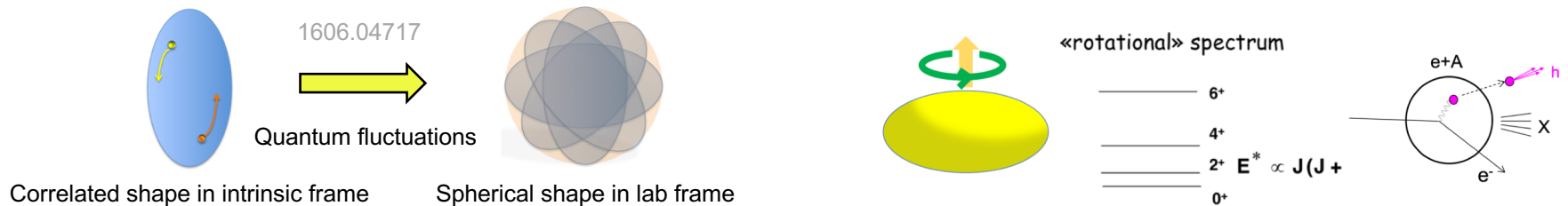


$$\langle \epsilon_2^2 \rangle \approx \langle \epsilon_0^2 \rangle + 0.2\beta_2^2$$

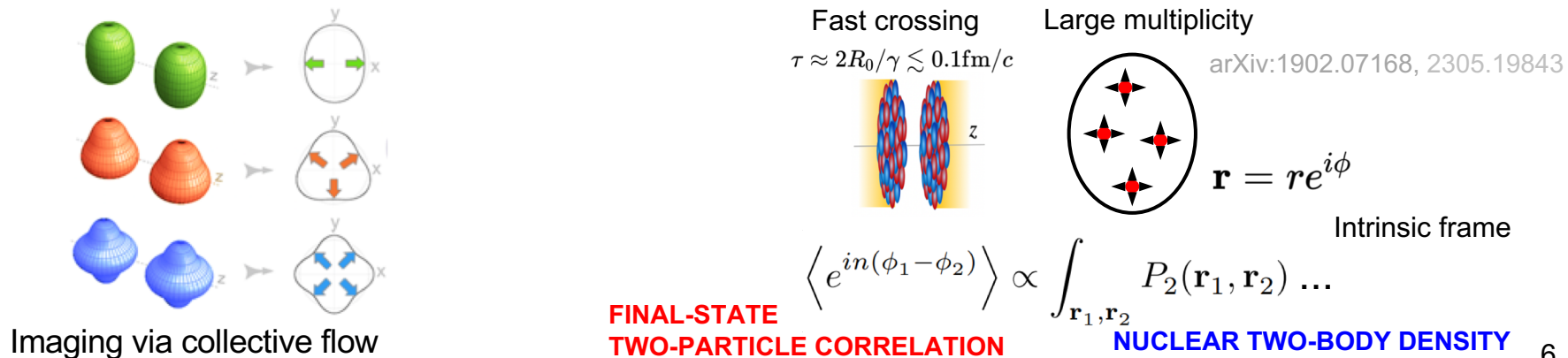
$$\langle v_n^2 \rangle \propto \langle \epsilon_n^2 \rangle \quad \text{In intrinsic frame}$$

Low-energy vs high-energy method

- Intrinsic frame shape not directly visible in lab frame at time scale $\tau > I/\hbar \sim 10^{-21} \text{ s}$
- Mainly inferred from largely “non-invasive” spectroscopic methods.



- High-energy collisions destructive imaging: probe entire mass distribution in the intrinsic frame via multi-point correlations. Shape frozen in nuclear crossing ($10^{-24} \text{ s} \ll$ rotational time scale 10^{-21} s)



Impact of nuclear shape on many-body correlations

$$\rho(r, \theta, \phi) = \frac{\rho_0}{1 + e^{(r-R(\theta, \phi))/a_0}} \quad R(\theta, \phi) = R_0(1 + \beta_2[\cos \gamma Y_{2,0}(\theta, \phi) + \sin \gamma Y_{2,2}(\theta, \phi)] + \beta_3 Y_{3,0}(\theta, \phi) + \beta_4 Y_{4,0}(\theta, \phi))$$

- In principle, can probe any moments of $p(1/R, \varepsilon_2, \varepsilon_3 \dots)$ via $p([p_T], v_2, v_3 \dots)$...

■ Mean	$\langle d_\perp \rangle$	$d_\perp \equiv 1/R_\perp$	$\langle p_T \rangle$
■ Variance:	$\langle \varepsilon_n^2 \rangle, \langle (\delta d_\perp / d_\perp)^2 \rangle$		$\langle v_n^2 \rangle, \langle (\delta p_T / p_T)^2 \rangle$
■ Skewness	$\langle \varepsilon_n^2 \delta d_\perp / d_\perp \rangle, \langle (\delta d_\perp / d_\perp)^3 \rangle$		$\langle v_n^2 \delta p_T / p_T \rangle, \langle (\delta p_T / p_T)^3 \rangle$
■ Kurtosis	$\langle \varepsilon_n^4 \rangle - 2\langle \varepsilon_n^2 \rangle^2, \langle (\delta d_\perp / d_\perp)^4 \rangle - 3\langle (\delta d_\perp / d_\perp)^2 \rangle^2$		$\langle v_n^4 \rangle - 2\langle v_n^2 \rangle^2, \langle (\delta p_T / p_T)^4 \rangle - 3\langle (\delta p_T / p_T)^2 \rangle^2$

...

- All have a simple connection to deformation:

- Variances

$$\begin{aligned} \langle \varepsilon_2^2 \rangle &\sim a_2 + b_2 \beta_2^2 + b_{2,3} \beta_3^2 \\ \langle \varepsilon_3^2 \rangle &\sim a_3 + b_3 \beta_3^2 \\ \langle \varepsilon_4^2 \rangle &\sim a_4 + b_4 \beta_4^2 \\ \langle (\delta d_\perp / d_\perp)^2 \rangle &\sim a_0 + b_0 \beta_2^2 + b_{0,3} \beta_3^2 \end{aligned}$$

- Skewness

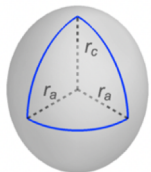
arXiv: 2109.00604

$$\begin{aligned} \langle \varepsilon_2^2 \delta d_\perp / d_\perp \rangle &\sim a_1 - b_1 \cos(3\gamma) \beta_2^3 \\ \langle (\delta d_\perp / d_\perp)^3 \rangle &\sim a_2 + b_2 \cos(3\gamma) \beta_2^3 \\ &\dots \end{aligned}$$

Example: Probing the nuclear three-body density (triaxiality)

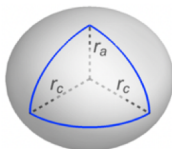
Prolate

$$\beta_2 = 0.25, \cos(3\gamma) = 1$$



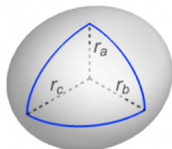
Triaxial

$$\beta_2 = 0.25, \cos(3\gamma) = 0$$



Oblate

$$\beta_2 = 0.25, \cos(3\gamma) = -1$$



$$R(\theta, \phi) = R_0 \left(1 + \beta_2 [\cos \gamma Y_{2,0} + \sin \gamma Y_{2,2}] \right)$$

G. Giuliano et.al 1910.04673, 2004.14463

tip-tip



small v_2
small area
large $[p_T]$

$$v_2 \searrow \quad p_T \nearrow$$

body-body



large v_2
large area
small $[p_T]$

$$v_2 \nearrow \quad p_T \searrow$$

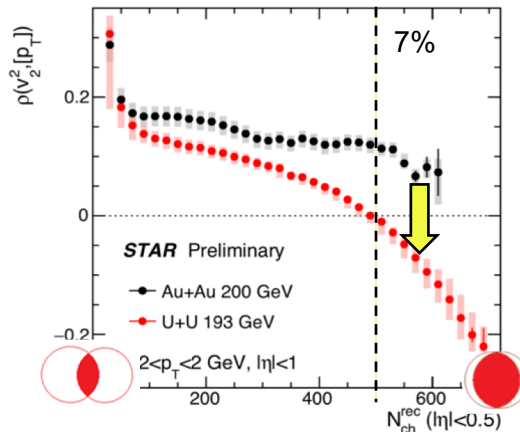
Need 3-point correlators to probe the 3 axes

$$\langle v_2^2 \delta p_T \rangle \sim -\beta_2^3 \cos(3\gamma)$$

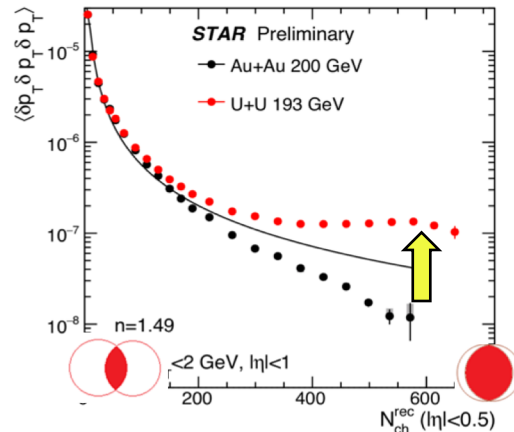
$$\langle (\delta p_T)^3 \rangle \sim \beta_2^3 \cos(3\gamma)$$

arXiv: 2109.00604

v_2 - $[p_T]$ covariance



$[p_T]$ skewness



Compare U+U vs Au+Au:

$$\beta_{2U} \sim 0.28, \beta_{2Au} \sim 0.13:$$

Strategy for nuclear shape imaging

Flow observable = **k** \otimes initial condition (structure)

 QGP response,
a smooth function of N+Z

 Structure of colliding nuclei,
non-monotonic function of N and Z

Compare two systems of similar size but different structure

$$R_{\mathcal{O}} \equiv \frac{\mathcal{O}_{\text{Ru}}}{\mathcal{O}_{\text{Zr}}} \approx 1 + c_1 \Delta \beta_2^2 + c_2 \Delta \beta_3^2 + c_3 \Delta R_0 + c_4 \Delta a \quad \text{arXiv: 2111.15559}$$

Deviation from unity depends only on their structure differences
 c_1 - c_4 are function of centrality

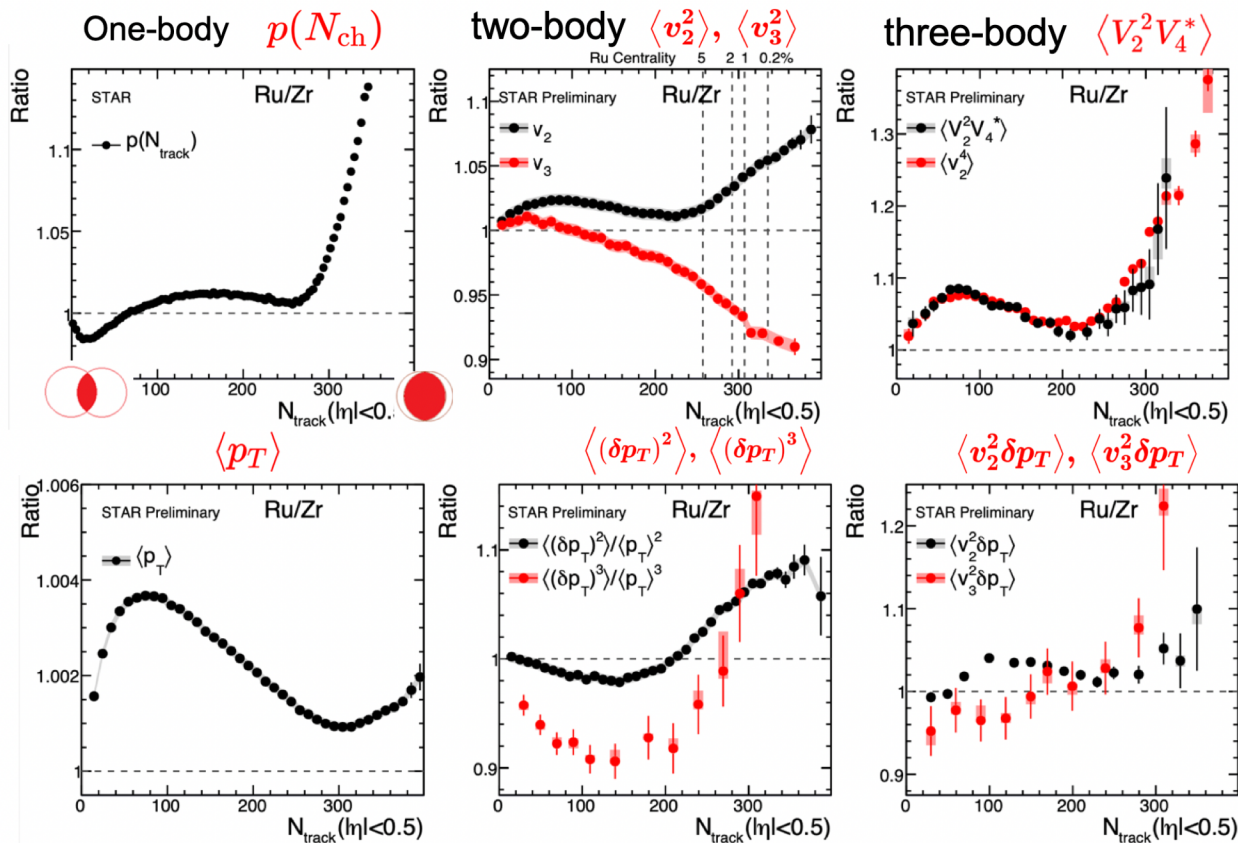
Isobar $^{96}\text{Ru}+^{96}\text{Ru}$ and $^{96}\text{Zr}+^{96}\text{Zr}$ collisions at RHIC 200 GeV

QM2022 poster, Chunjian Zhang

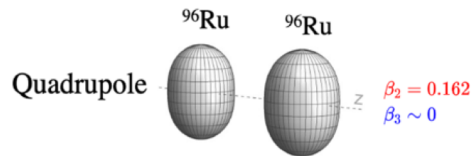
$$R_{\mathcal{O}} \equiv \frac{\mathcal{O}_{\text{Ru}}}{\mathcal{O}_{\text{Zr}}}$$

Structure influences
everywhere

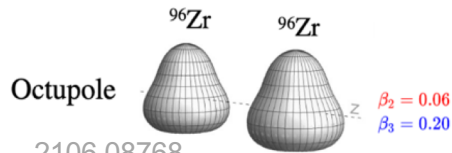
Nuclear structure is
inherently part of
Heavy ion problem



Nuclear structure via v_2 -ratio and v_3 -ratio

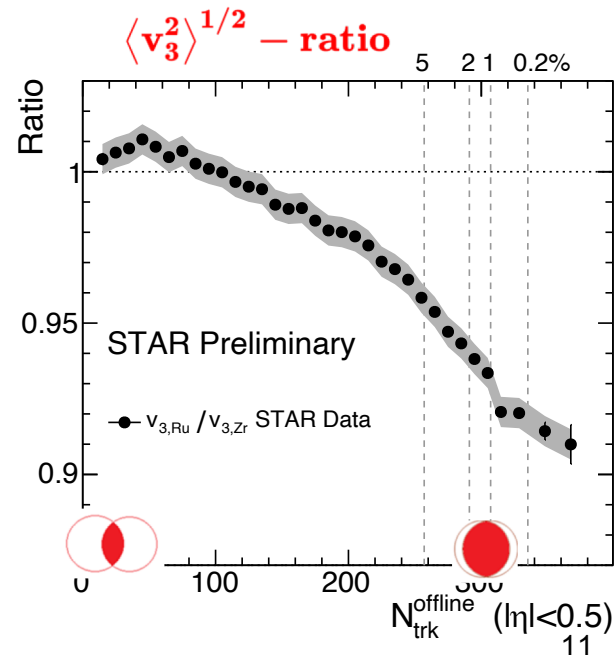
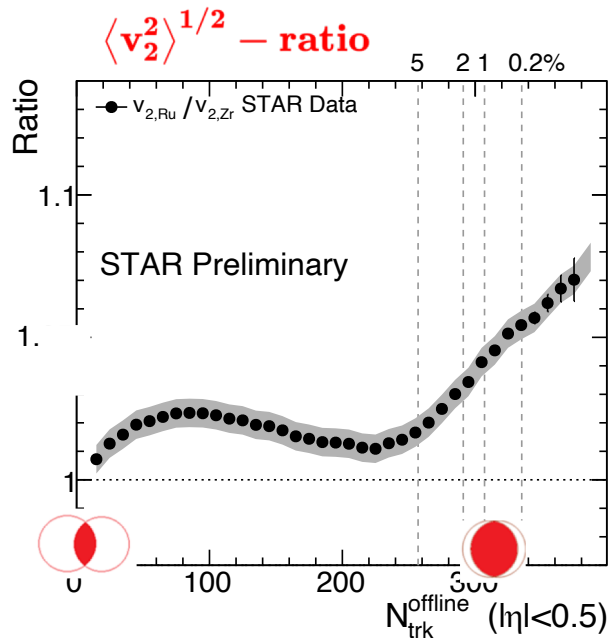


$$R_{\mathcal{O}} \equiv \frac{\mathcal{O}_{\text{Ru}}}{\mathcal{O}_{\text{Zr}}} \approx 1 + c_1 \Delta\beta_2^2 + c_2 \Delta\beta_3^2 + c_3 \Delta R_0 + c_4 \Delta a \quad 2109.00131$$

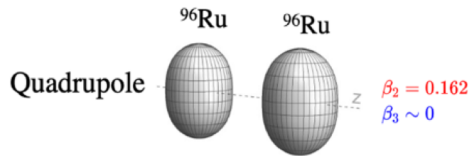


Simultaneously constrain four structure parameters

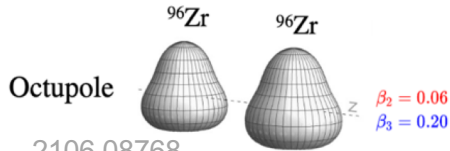
Species	β_2	β_3	a_0	R_0
Ru	0.162	0	0.46 fm	5.09 fm
Zr	0.06	0.20	0.52 fm	5.02 fm
difference	$\Delta\beta_2^2$	$\Delta\beta_3^2$	Δa_0	ΔR_0
	0.0226	-0.04	-0.06 fm	0.07 fm



Nuclear structure via v_2 -ratio and v_3 -ratio



$$R_{\mathcal{O}} \equiv \frac{\mathcal{O}_{\text{Ru}}}{\mathcal{O}_{\text{Zr}}} \approx 1 + c_1 \Delta\beta_2^2 + c_2 \Delta\beta_3^2 + c_3 \Delta R_0 + c_4 \Delta a \quad 2109.00131$$

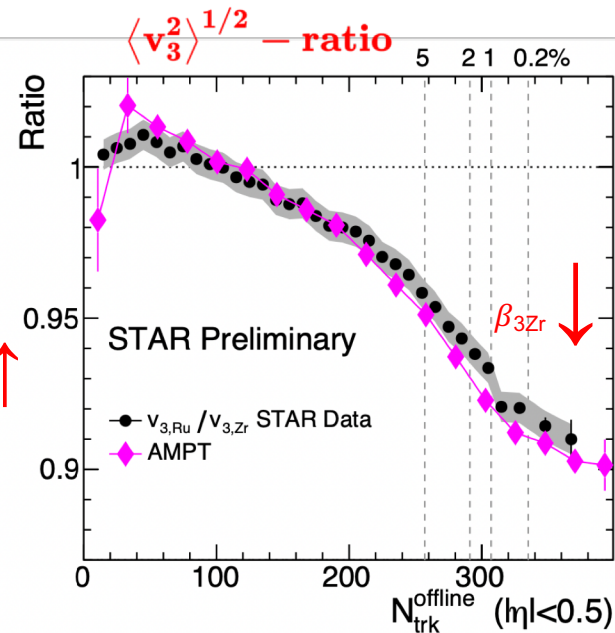
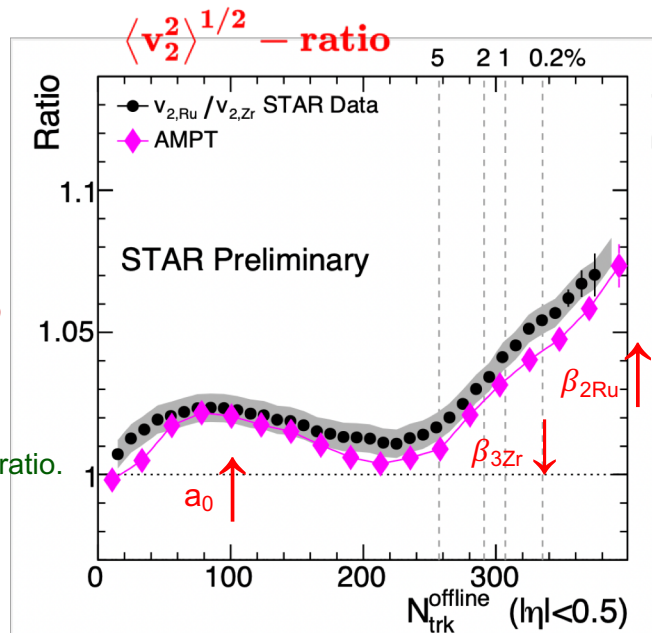


Simultaneously constrain four structure parameters

Species	β_2	β_3	a_0	R_0
Ru	0.162	0	0.46 fm	5.09 fm
Zr	0.06	0.20	0.52 fm	5.02 fm
difference	$\Delta\beta_2^2$	$\Delta\beta_3^2$	Δa_0	ΔR_0
	0.0226	-0.04	-0.06 fm	0.07 fm

- $\beta_{2\text{Ru}} \sim 0.16$ increase v_2 , no influence on v_3 ratio
- $\beta_{3\text{Zr}} \sim 0.2$ decrease v_2 and v_3 ratio
- $\Delta a_0 = -0.06$ fm increase v_2 mid-central,
- Radius $\Delta R_0 = 0.07$ fm slightly affects v_2 and v_3 ratio.

Is ^{96}Zr octupole deformed?



Isobar ratios cancel final state effects

- Vary the shear viscosity by changing partonic cross-section in AMPT

- Flow signal change by 30-50%, the v_n ratio unchanged.

$$v_n = k_n \varepsilon_n$$

↓

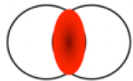
$$\frac{v_{n,Ru}}{v_{n,Zr}} \approx \frac{\varepsilon_{n,Ru}}{\varepsilon_{n,Zr}}$$

Robust probe of
initial state!

Nuclear structure

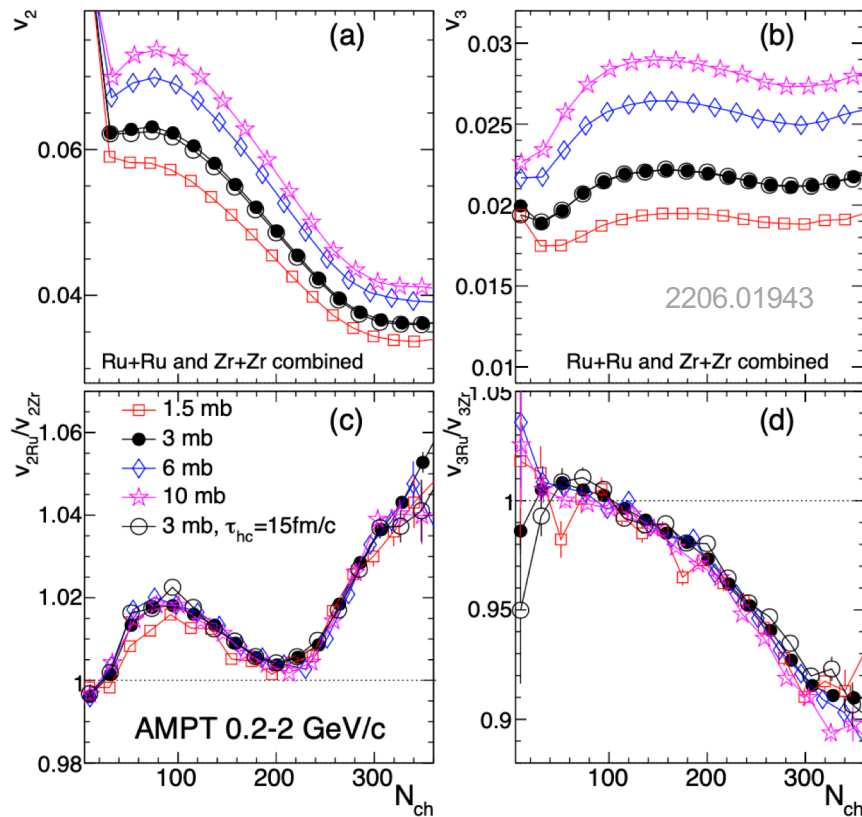


Initial condition



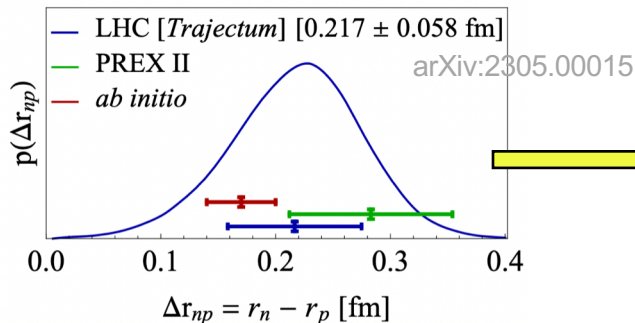
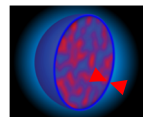
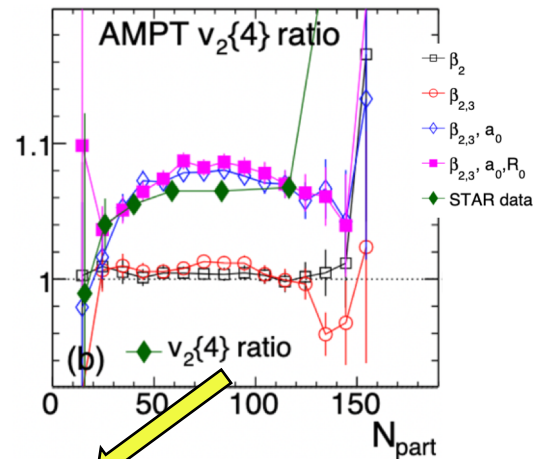
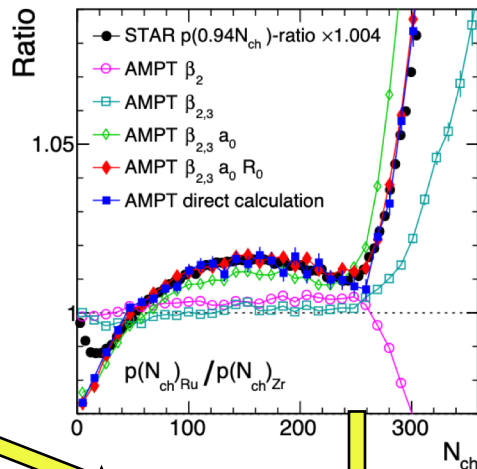
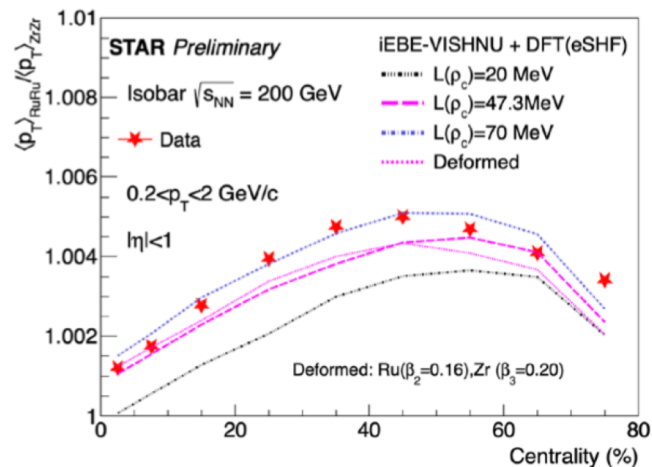
hydro

Final state

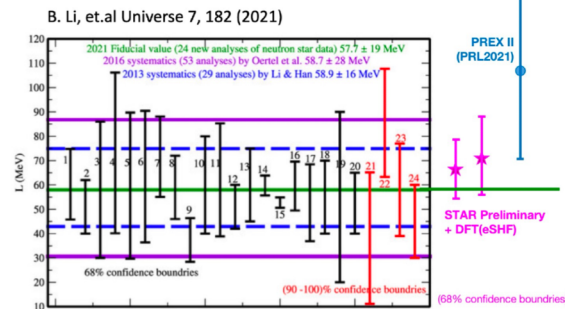


Imaging the radial structures \rightarrow neutron skin

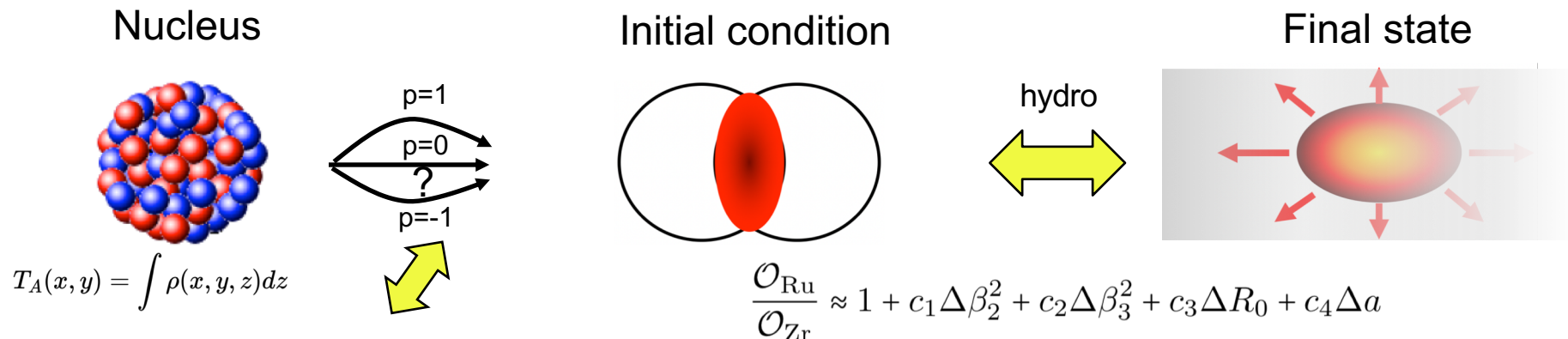
- Radial parameters R_0 , a_0 are properties of one-body distribution $\rightarrow \langle p_T \rangle$, $\langle N_{ch} \rangle$, $v_2^{RP} \sim v_2\{4\}$, σ_{tot}



Constrain neutron skin and symmetry energy



Constrain the heavy-ion initial condition



c_n relates nuclear structure and initial condition

- Different ways of depositing energy $T \propto \left(\frac{T_A^p + T_B^p}{2} \right)^{q/p}$

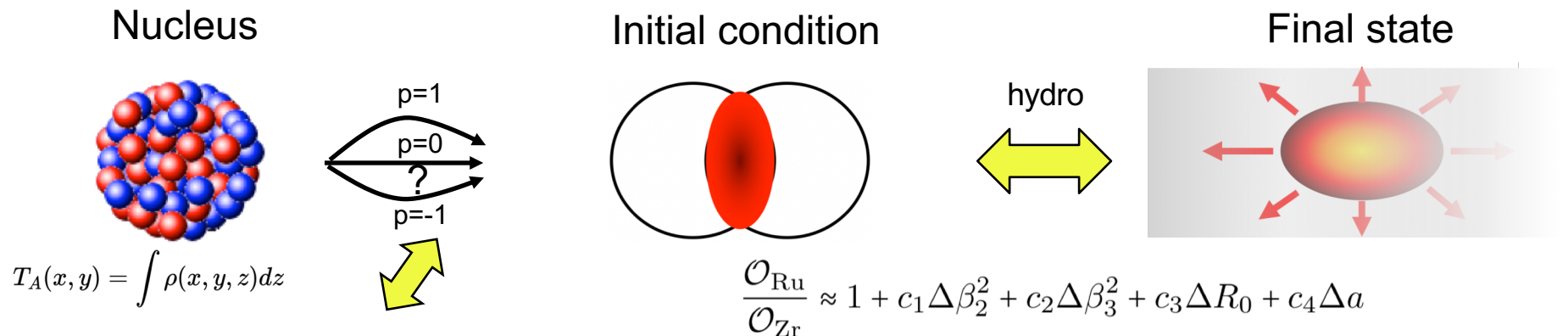
$$e(x, y) \sim \begin{cases} T_A + T_B & N_{\text{part}} - \text{scaling}, p = 1 \\ T_A T_B & N_{\text{coll}} - \text{scaling}, p = 0, q = 2 \\ \sqrt{T_A T_B} & \text{Trento default}, p = 0 \\ \min\{T_A, T_B\} & \text{KLN model}, p \sim -2/3 \\ T_A + T_B + \alpha T_A T_B & \text{two-component model,} \\ & \text{similar to quark-gluon model} \end{cases}$$

Other parameters:

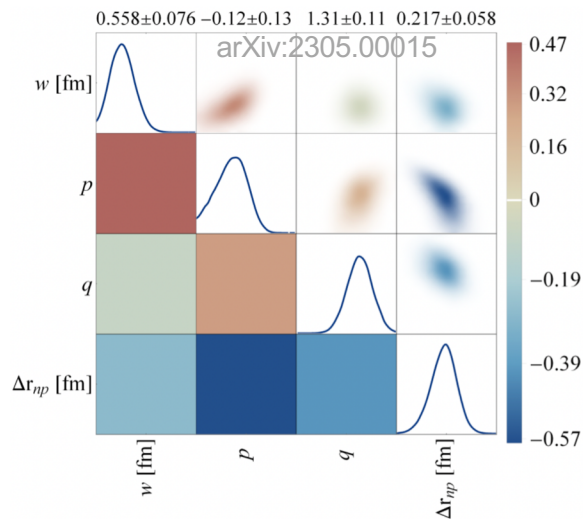
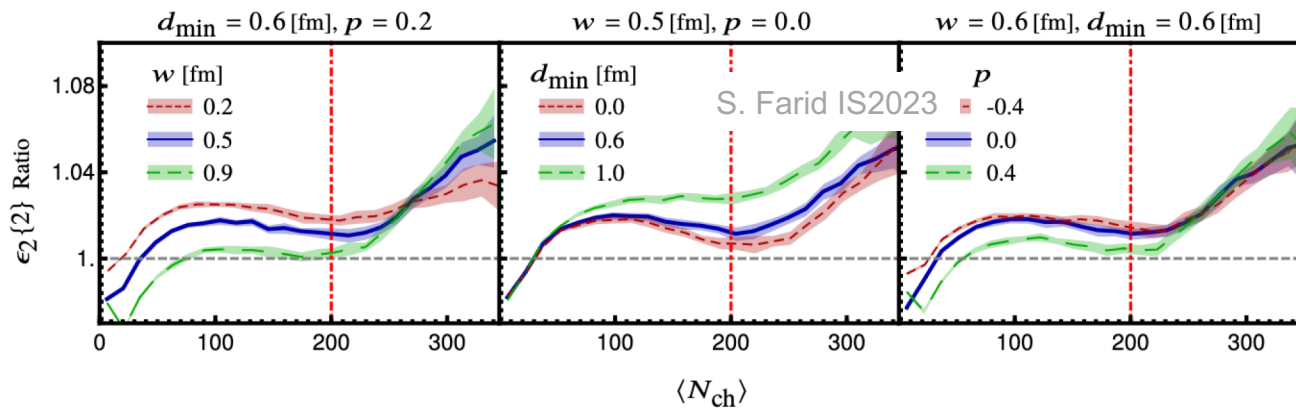
Nucleon width, w
 Minimum distance, d_{min} .
 Fluctuation parameter, σ_{fluc}

Use nuclear structure as extra lever-arm for initial condition

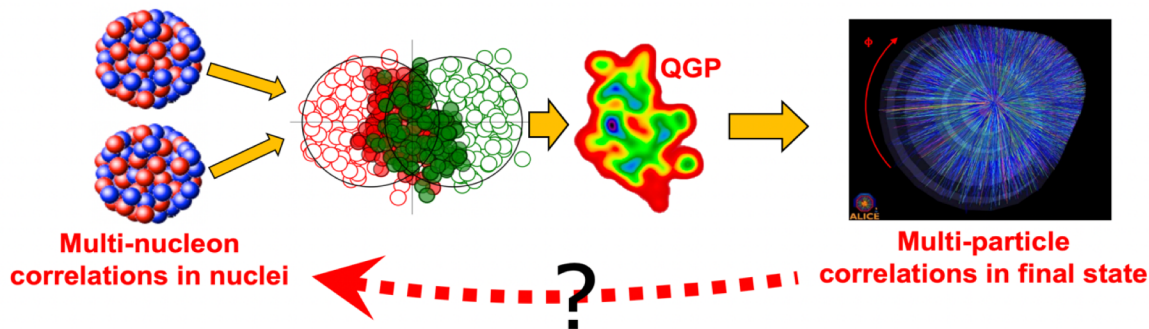
Constrain the heavy-ion initial condition



c_n relates nuclear structure and initial condition



Opportunities at the intersection of nuclear structure and hot QCD



Many examples in <https://arxiv.org/abs/2209.11042>

III. Science cases at the intersection of nuclear structure and hot QCD

- A. Stress-testing small system collectivity with ^{20}Ne
- B. Shape evolution along the Samarium isotopic chain
- C. The neutron skin of ^{48}Ca and ^{208}Pb in high-energy collisions
- D. Initial conditions of heavy-ion collisions
- E. Impact on future experiments: EIC and CBM FAIR

See recent [INT program 23-1A](#)

.....

New tests of effective field theories of low-energy QCD!

Summary and outlook

- High-energy collisions image nuclear shape at ultra-short time scale of 10^{-24} s; Large particle multiplicity enables many-particle correlation event-by-event to probe many-nucleon correlations in nuclei.
- Collisions of carefully-selected isobar species (at LHC) can reveal the many-body nucleon correlations & constrain the heavy ion initial condition from small to large nuclei

2102.08158

A	isobars	A	isobars	A	isobars	A	isobars	A	isobars	A	isobars
36	Ar, S	80	Se, Kr	106	Pd, Cd	124	Sn, Te, Xe	148	Nd, Sm	174	Yb, Hf
40	Ca, Ar	84	Kr, Sr, Mo	108	Pd, Cd	126	Te, Xe	150	Nd, Sm	176	Yb, Lu, Hf
46	Ca, Ti	86	Kr, Sr	110	Pd, Cd	128	Te, Xe	152	Sm, Gd	180	Hf, W
48	Ca, Ti	87	Rb, Sr	112	Cd, Sn	130	Te, Xe, Ba	154	Sm, Gd	184	W, Os
50	Ti, V, Cr	92	Zr, Nb, Mo	113	Cd, In	132	Xe, Ba	156	Gd, Dy	186	W, Os
54	Cr, Fe	94	Zr, Mo	114	Cd, Sn	134	Xe, Ba	158	Gd, Dy	187	Re, Os
64	Ni, Zn	96	Zr, Mo, Ru	115	In, Sn	136	Xe, Ba, Ce	160	Gd, Dy	190	Os, Pt
70	Zn, Ge	98	Mo, Ru	116	Cd, Sn	138	Ba, La, Ce	162	Dy, Er	192	Os, Pt
74	Ge, Se	100	Mo, Ru	120	Sn, Te	142	Ce, Nd	164	Dy, Er	196	Pt, Hg
76	Ge, Se	102	Ru, Pd	122	Sn, Te	144	Nd, Sm	168	Er, Yb	198	Pt, Hg
78	Se, Kr	104	Ru, Pd	123	Sb, Te	146	Nd, Sm	170	Er, Yb	204	Hg, Pb

Recently organized activities:

RBRC workshop Jan 2022, [link](#)

EMMI Taskforce May&Oct 2022, [link](#)

ESNT workshop Sep 2022, [link](#)

INT program Jan-Feb2023 [link](#)

Dalian workshop Aug 2023 [link](#)

Beijing workshop April 2024, in preparation

...